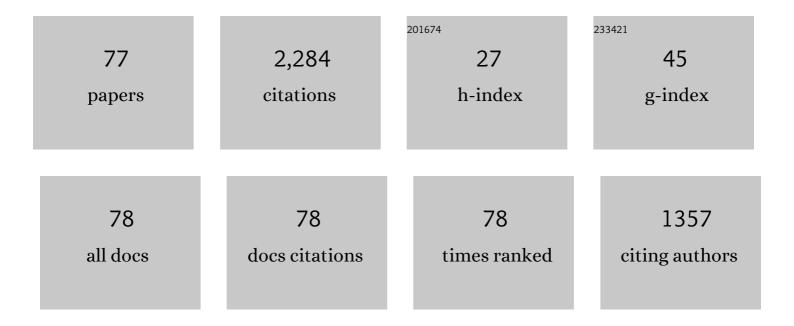
List of Publications by Year in descending order

Source: https://exaly.com/author-pdf/1433237/publications.pdf Version: 2024-02-01



#	Article	IF	CITATIONS
1	Burning plasma achieved in inertial fusion. Nature, 2022, 601, 542-548.	27.8	233
2	Nanosecond formation of diamond and lonsdaleite by shock compression of graphite. Nature Communications, 2016, 7, 10970.	12.8	167
3	Symmetry control of an indirectly driven high-density-carbon implosion at high convergence and high velocity. Physics of Plasmas, 2017, 24, .	1.9	106
4	The high velocity, high adiabat, "Bigfoot―campaign and tests of indirect-drive implosion scaling. Physics of Plasmas, 2018, 25, .	1.9	90
5	Design of inertial fusion implosions reaching the burning plasma regime. Nature Physics, 2022, 18, 251-258.	16.7	87
6	High-Performance Indirect-Drive Cryogenic Implosions at High Adiabat on the National Ignition Facility. Physical Review Letters, 2018, 121, 135001.	7.8	86
7	A measurement of the equation of state of carbon envelopes of white dwarfs. Nature, 2020, 584, 51-54.	27.8	70
8	X-ray scattering measurements on imploding CH spheres at the National Ignition Facility. Physical Review E, 2016, 94, 011202.	2.1	64
9	Characterizing the ionization potential depression in dense carbon plasmas with high-precision spectrally resolved x-ray scattering. Plasma Physics and Controlled Fusion, 2019, 61, 014015.	2.1	63
10	Improved Performance of High Areal Density Indirect Drive Implosions at the National Ignition Facility using a Four-Shock Adiabat Shaped Drive. Physical Review Letters, 2015, 115, 105001.	7.8	58
11	Achieving record hot spot energies with large HDC implosions on NIF in HYBRID-E. Physics of Plasmas, 2021, 28, .	1.9	55
12	Probing matter at Gbar pressures at the NIF. High Energy Density Physics, 2014, 10, 27-34.	1.5	52
13	Hotspot conditions achieved in inertial confinement fusion experiments on the National Ignition Facility. Physics of Plasmas, 2020, 27, .	1.9	50
14	High-speed three-dimensional plasma temperature determination of axially symmetric free-burning arcs. Journal Physics D: Applied Physics, 2013, 46, 125203.	2.8	46
15	Hot-spot mix in large-scale HDC implosions at NIF. Physics of Plasmas, 2020, 27, .	1.9	46
16	Generation and Beaming of Early Hot Electrons onto the Capsule in Laser-Driven Ignition Hohlraums. Physical Review Letters, 2016, 116, 075003.	7.8	45
17	Mixing in ICF implosions on the National Ignition Facility caused by the fill-tube. Physics of Plasmas, 2020, 27, .	1.9	41
18	Time-resolved measurements of the hot-electron population in ignition-scale experiments on the National Ignition Facility (invited). Review of Scientific Instruments, 2014, 85, 11D501.	1.3	39

#	Article	IF	CITATIONS
19	Absolute Equation-of-State Measurement for Polystyrene from 25 to 60ÂMbar Using a Spherically Converging Shock Wave. Physical Review Letters, 2018, 121, 025001.	7.8	39
20	Resolving hot spot microstructure using x-ray penumbral imaging (invited). Review of Scientific Instruments, 2016, 87, 11E201.	1.3	38
21	Performance of indirectly driven capsule implosions on the National Ignition Facility using adiabat-shaping. Physics of Plasmas, 2016, 23, 056303.	1.9	38
22	Examining the radiation drive asymmetries present in the high foot series of implosion experiments at the National Ignition Facility. Physics of Plasmas, 2017, 24, .	1.9	31
23	Thermal Temperature Measurements of Inertial Fusion Implosions. Physical Review Letters, 2018, 121, 085001.	7.8	31
24	Review of hydrodynamic instability experiments in inertially confined fusion implosions on National Ignition Facility. Plasma Physics and Controlled Fusion, 2020, 62, 014007.	2.1	31
25	First results of radiation-driven, layered deuterium-tritium implosions with a 3-shock adiabat-shaped drive at the National Ignition Facility. Physics of Plasmas, 2015, 22, .	1.9	29
26	Understanding the effects of radiative preheat and self-emission from shock heating on equation of state measurement at 100s of Mbar using spherically converging shock waves in a NIF hohlraum. Matter and Radiation at Extremes, 2020, 5, .	3.9	29
27	Symmetric fielding of the largest diamond capsule implosions on the NIF. Physics of Plasmas, 2020, 27, .	1.9	28
28	Experimental results of radiation-driven, layered deuterium-tritium implosions with adiabat-shaped drives at the National Ignition Facility. Physics of Plasmas, 2016, 23, .	1.9	27
29	Implosion performance of subscale beryllium capsules on the NIF. Physics of Plasmas, 2019, 26, 052707.	1.9	26
30	Hotspot parameter scaling with velocity and yield for high-adiabat layered implosions at the National Ignition Facility. Physical Review E, 2020, 102, 023210.	2.1	25
31	Localized mix-induced radiative cooling in a capsule implosion at the National Ignition Facility. Physical Review E, 2020, 101, 033205.	2.1	25
32	Absolute Hugoniot measurements from a spherically convergent shock using x-ray radiography. Review of Scientific Instruments, 2018, 89, 053505.	1.3	24
33	Note: A monoenergetic proton backlighter for the National Ignition Facility. Review of Scientific Instruments, 2015, 86, 116104.	1.3	23
34	Qualification of a high-efficiency, gated spectrometer for x-ray Thomson scattering on the National Ignition Facility. Review of Scientific Instruments, 2014, 85, 11D617.	1.3	22
35	Integrated performance of large HDC-capsule implosions on the National Ignition Facility. Physics of Plasmas, 2020, 27, .	1.9	22
36	Simulating x-ray Thomson scattering signals from high-density, millimetre-scale plasmas at the National Ignition Facility. Physics of Plasmas, 2014, 21, .	1.9	21

#	Article	IF	CITATIONS
37	Mix and hydrodynamic instabilities on NIF. Journal of Instrumentation, 2017, 12, C06001-C06001.	1.2	21
38	A near one-dimensional indirectly driven implosion at convergence ratio 30. Physics of Plasmas, 2018, 25, .	1.9	20
39	Achieving 280 Gbar hot spot pressure in DT-layered CH capsule implosions at the National Ignition Facility. Physics of Plasmas, 2020, 27, .	1.9	20
40	Observation of Hydrodynamic Flows in Imploding Fusion Plasmas on the National Ignition Facility. Physical Review Letters, 2021, 127, 125001.	7.8	20
41	Application of cross-beam energy transfer to control drive symmetry in ICF implosions in low gas fill <i>Hohlraums</i> at the National Ignition Facility. Physics of Plasmas, 2020, 27, .	1.9	18
42	In situ droplet surface tension and viscosity measurements in gas metal arc welding. Journal Physics D: Applied Physics, 2012, 45, 175202.	2.8	16
43	Using penumbral imaging to measure micrometer size plasma hot spots in Gbar equation of state experiments on the National Ignition Facility. Review of Scientific Instruments, 2014, 85, 11D614.	1.3	16
44	X-ray Thomson scattering as a temperature probe for Gbar shock experiments. Journal of Physics: Conference Series, 2014, 500, 192019.	0.4	16
45	Shock Hugoniot measurements of CH at Gbar pressures at the NIF. Journal of Physics: Conference Series, 2016, 688, 012055.	0.4	16
46	Platform for spectrally resolved x-ray scattering from imploding capsules at the National Ignition Facility. Journal of Physics: Conference Series, 2016, 717, 012067.	0.4	16
47	Physics of Plasmas, 2015, 22, 056307.	1.9	14
48	eHXI: a permanently installed, hard x-ray imager for the National Ignition Facility. Journal of Instrumentation, 2016, 11, P06010-P06010.	1.2	14
49	A boundary condition for Guderley's converging shock problem. Physics of Fluids, 2019, 31, .	4.0	12
50	Deficiencies in compression and yield in x-ray-driven implosions. Physics of Plasmas, 2020, 27, .	1.9	12
51	Experiments to explore the influence of pulse shaping at the National Ignition Facility. Physics of Plasmas, 2020, 27, 112708.	1.9	11
52	An x-ray penumbral imager for measurements of electron–temperature profiles in inertial confinement fusion implosions at OMEGA. Review of Scientific Instruments, 2021, 92, 043548.	1.3	10
53	On the design of the NIF Continuum Spectrometer. , 2017, , .		9
54	Recent and planned hydrodynamic instability experiments on indirect-drive implosions on the National Ignition Facility. High Energy Density Physics, 2020, 36, 100820.	1.5	8

#	Article	lF	CITATIONS
55	Demonstration of a laser-driven, narrow spectral bandwidth x-ray source for collective x-ray scattering experiments. Physics of Plasmas, 2021, 28, .	1.9	8
56	Using neutrons to measure keV temperatures in highly compressed plastic at multi-Gbar pressures. High Energy Density Physics, 2016, 21, 20-26.	1.5	7
57	Principal factors in performance of indirect-drive laser fusion experiments. Physics of Plasmas, 2020, 27, .	1.9	7
58	Measurements of enhanced performance in an indirect drive inertial confinement fusion experiment when reducing the contact area of the capsule support. Physics of Plasmas, 2020, 27, .	1.9	7
59	X-ray penumbral imaging diagnostic developments at the National Ignition Facility. , 2017, , .		7
60	New Methods to Look at an Old Technology: Innovations to Diagnose Thermal Plasmas. Plasma Chemistry and Plasma Processing, 2015, 35, 437-453.	2.4	6
61	Improving a high-efficiency, gated spectrometer for x-ray Thomson scattering experiments at the National Ignition Facility. Review of Scientific Instruments, 2016, 87, 11E515.	1.3	6
62	Beryllium implosions at smaller case-to-capsule ratio on NIF. High Energy Density Physics, 2020, 34, 100747.	1.5	6
63	Hot Spot Evolution Measured by High-Resolution X-Ray Spectroscopy at the National Ignition Facility. Physical Review Letters, 2022, 128, 185002.	7.8	6
64	X-ray continuum emission spectroscopy from hot dense matter at Gbar pressures. Review of Scientific Instruments, 2014, 85, 11D606.	1.3	5
65	Using time-resolved penumbral imaging to measure low hot spot x-ray emission signals from capsule implosions at the National Ignition Facility. Review of Scientific Instruments, 2018, 89, 10G111.	1.3	5
66	Investigation of the temperature in dense carbon near the solid-liquid phase transition between 100ÂGPa and 200ÂGPa with spectrally resolved X-ray scattering. High Energy Density Physics, 2019, 32, 56-62.	1.5	5
67	Optimization of capsule dopant levels to improve fuel areal density*. High Energy Density Physics, 2020, 37, 100884.	1.5	5
68	Three-dimensional electron temperature measurement of inertial confinement fusion hotspots using x-ray emission tomography. Review of Scientific Instruments, 2022, 93, .	1.3	5
69	Measurement of high-dynamic range x-ray Thomson scattering spectra for the characterization of nano-plasmas at LCLS. Review of Scientific Instruments, 2016, 87, 11E709.	1.3	4
70	Improved hard x-ray (50-80 keV) imaging of hohlraum implosion experiments at the National Ignition Facility. Proceedings of SPIE, 2016, , .	0.8	4
71	Hydroscaling indirect-drive implosions on the National Ignition Facility. Physics of Plasmas, 2022, 29, .	1.9	4
72	Session 2: Microfluidics and nanotechnology. Journal of Labelled Compounds and Radiopharmaceuticals, 2009, 52, S8-S14.	1.0	3

#	Article	IF	CITATIONS
73	Dual crystal x-ray spectrometer at 1.8 keV for high repetition-rate single-photon counting spectroscopy experiments. Journal of Instrumentation, 2016, 11, P08015-P08015.	1.2	2
74	Simultaneous compression and opacity data from time-series radiography with a Lagrangian marker. Review of Scientific Instruments, 2021, 92, 063514.	1.3	2
75	Bound on hot-spot mix in high-velocity, high-adiabat direct-drive cryogenic implosions based on comparison of absolute x-ray and neutron yields. Physical Review E, 2022, 106, .	2.1	2
76	Using neutrons and x rays to measure plasma conditions in a solid sphere of deuterated polyethylene compressed to densities of 35 g/cc at temperatures of 2 keV and pressures of 40 Gbar. Physics of Plasmas, 2021, 28, .	1.9	1
77	Performance of indirectly driven capsule implosions on NIF using adiabat-shaping. Journal of Physics: Conference Series, 2016, 717, 012045.	0.4	Ο